DOI: 10.1002/cbic.200900071

Parallel Pathways and Free-Energy Landscapes for Enzymatic Hydride Transfer Probed by Hydrostatic Pressure

Christopher R. Pudney,[a] Tom McGrory,[b] Pierre Lafite,[a] Jiayun Pang,[b] Sam Hay,[a] David Leys,[a] Michael J. Sutcliffe,[b] and Nigel S. Scrutton*[a]

We show that hydride transfer from NADH to FMN catalysed by the N189A mutant of morphinone reductase occurs along parallel "chemical" pathways in a conformationally rich free-energy landscape. We have developed experimental kinetic and spectroscopic tools by using hydrostatic pressure to explore this free-energy landscape. The crystal structure of the N189A mutant enzyme in complex with the unreactive coenzyme analogue $NADH_4$ indicates that the nicotinamide moiety of the analogue is conformationally less restrained than the corresponding structure of the wild-type $NADH_4$ complex. This increased degree of conformational freedom in the N189A enzyme gives rise to the concept of multiple reactive configurations (MRCs), and we show that the relative population of these states across the free-energy landscape can be perturbed experimentally as a function of pressure. Specifically, the amplitudes of individual kinetic phases that were observed in stopped-flow studies of the hydride transfer reaction are sensitive to pressure; this indicates that pressure drives an altered distribution across the energy landscape. We show by absorbance spectroscopy that the loss of charge-transfer character of the enzyme–coenzyme complex is attributed to the altered population of MRCs on the landscape. The existence of a conformationally rich landscape in the N189A mutant is supported by molecular dynamics simulations at low and high pressure. The work provides firm experimental and computational support for the existence of parallel pathways arising from multiple conformational states of the enzyme–coenzyme complex. Hydrostatic pressure is a powerful and general probe of multidimensional energy landscapes that can be used to analyse experimentally parallel pathways for enzyme-catalysed reactions. We suggest that this is especially the case following directed mutation of a protein, which can lead to increased population of reactant states that are essentially inaccessible in the free-energy landscape of wild-type enzyme.

Introduction

Proteins are fluctuating, dynamic systems and are able to assume a large number of nearly isoenergetic low-energy conformational substates.[1–3] Each of these exists in thermal equilibrium, and so may interconvert. A consequence is that proteins are now commonly thought of as fluctuating free-energy landscapes, capable of populating (transiently) these nearly isoenergetic minima. This is consistent with single-molecule studies[4–6] and atomistic simulations[7,8] that point to free-energy landscapes for enzyme–substrate complexes with multiple reactant states and paths. Reactive configurations that correspond to landscape minima are each capable of productive catalysis by proceeding via the same reaction chemistry, but the microscopic rate constant for each reaction will differ across these reactant configurations. Consequently, the rate enhancements achieved by enzymes are a statistically weighted average of a diverse population of rate constants spanning several orders of magnitude.

There is now increased recognition of the contributions made by multiple reactant states and paths to the overall observed rate of an enzymatic reaction.[9] A number of examples exist in which the contribution of different conformational substates are inferred: examples include dihydrofolate reductase (DHFR),[8] thermophilic alcohol dehydrogenase (tmADH)[10] and dihydroorotate dehydrogenase (DHOD).[4] However, it remains difficult to monitor conformational substates experimentally, let alone perturb them. We have previously studied the reductive half-reaction (RHR) of wild-type morphinone reductase (MR) in detail.[11–13] The RHR involves hydride transfer from the C4 *R* hydrogen of β-nicotinamide adenine dinucleotide (NADH) to the N5 atom of flavin mononucleotide (FMN). The RHR proceeds in three steps and H-transfer—which is concomitant with FMN reduction—is kinetically resolved from the preceding steps involving coenzyme binding and formation of the MR–NADH binary complex:

FMN reduction is observed directly in a rapid-mixing, stopped-flow instrument by following the decrease in absorbance at 464 nm. Also the binary complex, $[MR{\cdot}NADH]^{CT}$, has a

[a] *Dr. C. R. Pudney, Dr. P. Lafite, Dr. S. Hay, Dr. D. Leys, Prof. N. S. Scrutton*
Faculty of Life Sciences and Manchester Interdisciplinary Biocentre
University of Manchester
131 Princess Street, Manchester, M1 7DN (UK)
Fax: (+44) 161-306-8918
E-mail: nigel.scrutton@manchester.ac.uk

[b] *T. McGrory, Dr. J. Pang, Prof. M. J. Sutcliffe*
School of Chemical Engineering and Analytical Science and
Manchester Interdisciplinary Biocentre, University of Manchester
131 Princess Street, Manchester, M1 7DN (UK)

Supporting information for this article is available on the WWW under http://dx.doi.org/10.1002/cbic.200900071.

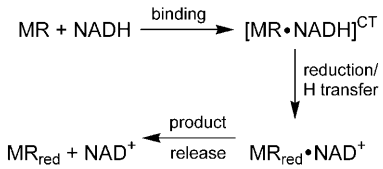

characteristic π–π absorbance centred at 555 nm, which is attributed to the formation of a charge-transfer (CT) complex.

In earlier work, we studied the MR active-site mutant N189A,[14] and showed that this mutation enables a number of conformational substates to be more significantly populated than in the wild-type enzyme. As a consequence, we were able to monitor a number of these substates, termed multiple reactive configurations (MRCs), by using stopped-flow methods. In particular, we observed a multiphasic absorption change at 466 nm for FMN reduction by NADH in N189A MR. This contrasts with the single phase observed with wild-type MR. The reaction transient for the N189A enzyme was fitted to a multiexponential function [Eq. (1)] with at least three rate constants.[14]

$$\Delta A = \sum_{i=1}^{\text{No. of states}} A_i \exp(-kt) \qquad (1)$$

Where A_i is the amplitude and k_i is the rate constant of the *i*th exponential component that was obtained from the stopped-flow trace, and ΔA is the total absorbance change. In this analysis each exponential component was considered to reflect a major reactive configuration, which has become kinetically accessible. We term these configurations R_1–R_3, respectively.[14] By using stable isotope analysis and thermodynamic and kinetic characterisations, we showed that each reactive configuration proceeds by the same chemical mechanism, but that the rate constants for hydride transfer to FMN varied by over three orders of magnitude (~200–0.2 s^{-1}).[14] Each of these reactive configurations may therefore be considered to represent parallel pathways for FMN reduction.

In this work, we have extended our analysis of the N189A mutant MR to explore the free-energy landscape for hydride transfer following pressure perturbation. We show that pressure perturbs the free-energy landscape for the N189A MR–NADH binary complex and causes the population of MRCs to shift significantly. X-ray crystallographic data support the concept of parallel reaction pathways induced by mutation of Asn189 and molecular dynamics simulations corroborate the experimental evidence for fluctuations in the free-energy landscape with pressure. We suggest that hydrostatic pressure is a powerful and general probe of multidimensional energy landscapes that can be used to analyse experimentally parallel pathways for enzyme-catalysed reactions. This is especially the case following directed mutagenesis of the active site, which can lead to increased population of reactant states that are essentially inaccessible in the free-energy landscape of wild-type enzymes.

Results and Discussion

Crystal structure of N189A MR–$NADH_4$ complex

We have previously reported the X-ray crystal structure of wild-type MR in complex with the non-reactive NADH analogue 1,4,5,6-tetrahydroNADH ($NADH_4$).[14] We have now determined the structure of N189A MR in complex with $NADH_4$ at a resolution of 2.3 Å (Figure 1 and Table S1 in the Supporting Information). The overall structure of N189A MR–$NADH_4$ is similar to that of the wild-type protein, although major differences are visible in the region A187–L192 (Figure 1). We modelled two conformations of this chain based on the observed electron density. One conformation corresponds to that in wild-type

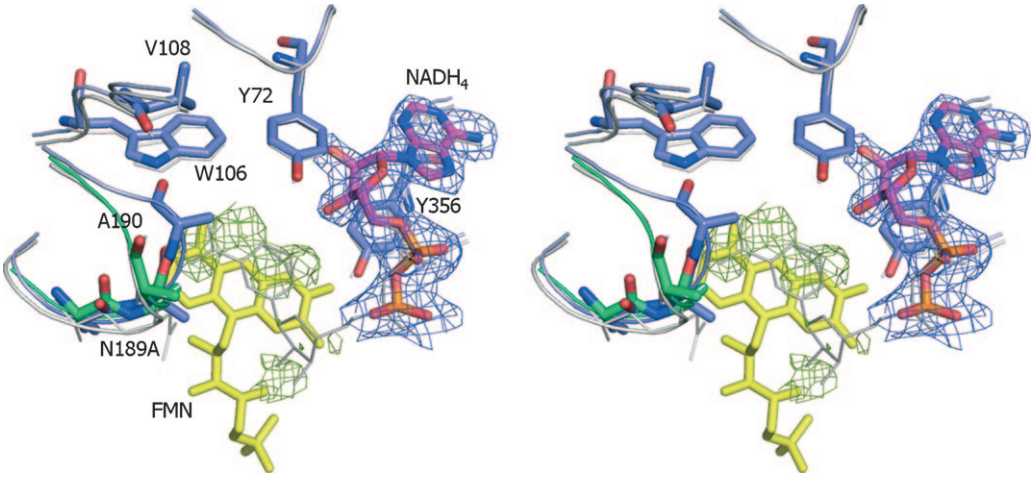

Figure 1. Stereoview of the N189A MR–$NADH_4$ complex overlaid with the wild-type MR–$NADH_4$ complex. For the mutant structure, selected residues in the active site as well as the bound FMN and $NADH_4$ are shown in atom-coloured sticks. For comparison, the corresponding wild-type structure is depicted in narrow grey-scale sticks. In the N189A MR structure, the loop containing the N189A mutation is observed in two distinct conformations and is coloured respectively with blue and green carbons (the latter similar of the wild-type structure). A section of the $2F_o-F_c$ electron density map corresponding to the ordered moiety of $NADH_4$ is shown as a blue mesh. A section of the residual F_o-F_c electron density map is shown as a green mesh situated above the FMN isoalloxazine ring. This could not be interpreted in terms of a single conformation of the $NADH_4$ nicotinamide moiety.

enzyme, whereas the second indicates displacement of the peptide toward residues W106 and Y72 (Figure 1). It is interesting to note that the latter conformation precludes a stacking of the $NADH_4$ nicotinamide with the FMN as seen in the wild-type enzyme. In case of the N189A MR mutant, unambiguous electron density is observed for the adenosine-phosphate moiety of the bound $NADH_4$ (Figure 1). In contrast, a region of less well-defined density is observed above the *si* face of the FMN isoalloxazine ring. We infer that this is attributed to a limited occupancy of the nicotinamide-ribose moiety of $NADH_4$ in this position, which is possibly linked to the position of the A187–L192 conformation. This clearly suggests mobility of the nicotinamide group when bound to N189A MR. This contrasts with the structure of the $NADH_4$-bound wild-type enzyme, in which the nicotinamide density is well defined.[14]

The structure of the N189A MR–$NADH_4$ complex is consistent with our previous kinetic and molecular dynamics analysis of hydride transfer from NADH to FMN in the N189A mutant MR.[14] We had suggested that during hydride transfer MRCs are populated as a consequence of removing the restraining interaction between the carboxamide group of NADH and Asn189. This is consistent with the localised disorder of the nicotinamide group in the N189A MR–$NADH_4$ complex and the well-defined position of the remaining adenosine-phosphate moiety of the coenzyme.

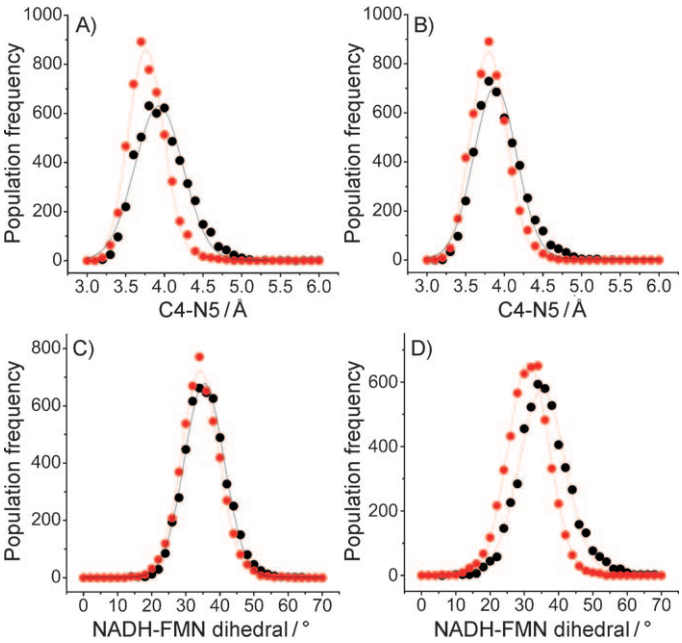

Figure 2. Molecular dynamics simulations of wild-type MR and N189A MR at 1 bar and 2 kbar. Data reported in the text are extracted from the centre of the Gaussian fits, which are shown as solid lines. Panels A and B show the variation in C4–N5 distance for wild-type (A) and N189A MR (B) at 1 bar (black) and 2 kbar (red). Distances were binned at 0.1 Å. Panels C and D show the NADH–FMN dihedral angle (NADH-N1–NADH-C4–FMN-N5–FMN-N10) for wild-type (A) and N189A MR (B) at 1 bar (black) and 2 kbar (red). Dihedral angles were binned at 2°.

High pressure molecular dynamics and energy landscapes for enzyme–NADH complexes

We performed high-pressure molecular dynamics (MD) simulations of wild-type and N189A MR in complex with NADH and FMN at 1 bar (1 bar = 100 kPa = 0.98 atm) and 2 kbar (RMSDs for 10 ns simulation shown in Figure S1) to 1) provide atomistic understanding of pressure-induced structural perturbation and 2) support experimental studies of hydride transfer kinetics in both enzymes as a function of pressure. The conformational states that we observe define the energy landscapes for the enzyme–NADH complexes of wild-type and N189A enzymes.

Our previous MD simulations of N189A MR at 1 bar suggested increased conformational freedom for the nicotinamide group compared to wild-type enzyme.[14] There is also a better overlap of the nicotinamide and isoalloxazine rings in a subset of conformations for the mutant enzyme. We have also shown with wild-type MR that on increasing the pressure from 1 bar to 2 kbar an equilibrium distribution of conformational states is favoured in which the average donor–acceptor distance (i.e., distance between the C4–N5 atoms of the nicotinamide coenzyme and FMN, respectively) is shortened.[15] We now extend this analysis to the N189A MR–NADH complex which allows comparison with the wild type MR–NADH complex. The simulations show that across the landscape the population frequency, and in particular the average C4-N5 distances, change with pressure for both wild-type and N189A MR (Figure 2A, B). The C4-N5 distance decreases for wild-type (3.93 to 3.74 Å) and N189A (3.88 to 3.77 Å) MR on moving from 1 bar to 2 kbar. We have monitored the change in dihedral angle (NADH N1-NADH C4-FMN N5-FMN N10) on moving from 1 bar to 2 kbar (Figures S2 and 2C, D). At 1 bar the dihedral is similar in wild-type MR compared to N189A MR being, $35.4 \pm 0.08^\circ$ and $35.2 \pm 0.12^\circ$, respectively. Further, at high pressure (2 kbar) the dihedral in wild-type MR and N189A MR is decreased, although to a greater extent with the mutant being, $34.2 \pm 0.06^\circ$ and $31.3 \pm 0.07^\circ$, respectively. These data therefore suggest that whilst the donor–acceptor distance is shorter in wild-type MR at high pressure, the relative position of the isoalloxazine and nicotinamide rings is more significantly different in N189A MR. These data might reflect the increased conformational freedom of N189A MR relative to wild-type MR.

Exploring the energy landscape by pressure perturbation of hydride-transfer chemistry in N189A MR

We showed previously that mutation of Asn189 to alanine resulted in complex kinetic behaviour in the reductive half-reaction of MR.[14] In stopped-flow studies of FMN reduction by NADH we observed three exponential phases in the kinetics of flavin reduction, each reflecting hydride transfer, and demonstrating hydride transfer occurs in a series of parallel reactions (cf. wild-type enzyme) for the reactive enzyme–coenzyme complex. We define this population of reactive conformations as MRCs. In reality, the number of reactive states will be greater than three, but detection of these is compromised by using ensemble stopped-flow measurements. We focus below on the experimentally observed states, but the general conclusions apply to all conformations of the enzyme–coenzyme complex.

By using our stopped-flow methods[14] we have analysed how the distribution across the MRCs in N189A MR–NADH varies with pressure. Any shift in the distribution of conformational states can be approximated in relative terms by the variation in amplitude of the individual exponential components corresponding to each MRC. Figure 3 shows the variation in amplitude and observed rate of FMN reduction for each of the kinetically accessible reactive configurations over the pressure range 1–2000 bar. These data are summarised in Table 1. The variation in population of a reactive configuration relative to other configurations may be modelled by using Equation (2):

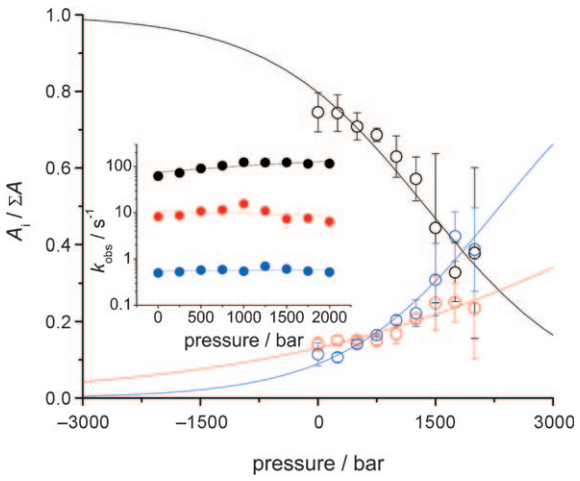

Figure 3. Pressure dependence of the relative amplitude and observed rate that was extracted from stopped-flow transients of the reductive half-reaction of N189A MR. The amplitude data were fitted to Equation (2) for each reactive configuration, black (R_1), red (R_2) and blue (R_3). The data are extrapolated to negative pressure values to demonstrate the properties of Equation (2). Inset: pressure dependence of the rate constants obtained by stopped-flow measurements for R_{1-3}. Solid lines in the main panel are fits to Equation (3). Conditions: N189A MR (75 μM) and NADH (40 mM) at 4 °C.

$$\frac{A_i}{\sum A}(p,T) = \frac{K_i(p,T)}{1+K_i(p,T)} = \frac{\exp(\ln K_{i,0} - \Delta V_A p/R_p T)}{1+\exp(\ln K_{i,0} - \Delta V_A p/R_p T)} \quad (2)$$

Here, $R_p = 83.13\ cm^3\,mol^{-1}\,bar\,K^{-1}$ when the pressure, p, is measured in bar, $K_{i,0}$ is the equilibrium constant for the change in population of the ith reactive configuration extrapolated to 0 bar and V_A is analogous to $V^{\neq}$ in Equation (3), being the apparent difference in the volume associated with this equilibrium transition.

From Figure 3 and Table 1 it is clear that the relative population of each of the MRCs is sensitive to changes in hydrostatic pressure. This is apparent from the variation in the amplitude of each configuration ($\Delta V_{A1} = 23.1 \pm 2.7$, $\Delta V_{A2} = -9.5 \pm 1.5$ and $\Delta V_{A3} = -23 \pm 2.5\ cm^3\,mol^{-1}$). In short, the amplitude data show that R_1 becomes less populated and R_{2-3} more populated as the pressure increases from 1–2000 bar. The pressure dependence of the observed rate constants for each MRC is extracted from Equation (3),[13]

Table 1. The pressure dependence of the amplitude and observed rate constant for each phase attributable to hydride transfer in N189A MR.

	K_0[a]	ΔV_A [$cm^3\,mol^{-1}$][b]	k_0 [s^{-1}][b]	$\Delta V^{\neq}$ [$cm^3\,mol^{-1}$][b]
N189A MR				
R_1	3.9 ± 0.6	23.1 ± 2.7	79.5 ± 8.1	−5.7 ± 1.7
R_2	0.15 ± 0.01	−9.5 ± 1.5	10.6 ± 1.9	2.4 ± 3.6
R_3	0.10 ± 0.02	−23.0 ± 2.5	0.55 ± 0.04	−0.8 ± 1.3
Wild-type MR[c]				
	–	–	18.3 ± 0.6	−14.39 ± 0.69

[a] Values were obtained by fitting the amplitude data to Equation 2, while [b] values are from linear fits of the rate constant data to Equation (3). All measurements were made at 4 °C in 50 mM Tris–HCl, 2 mM 2-mercaptoethanol, 5 U mL^{-1} glucose oxidase, 50 mM glucose, pH 8.0 and were measured at 466 nm on a log time scale over 20 or 50 s with ~8000 data points and fitted to 3-exponentials by using Kinetic Studio. Concentration used: 75 μM MR N189A vs. 40 mM (final concentrations) NADH and wild-type MR vs. 5 mM (final concentrations) NADH. [c] Data from Hay et al.[13]

$$k_{obs}(p,T) = k_0 \exp(-\Delta V^{\neq} p/R_p T) \quad (3)$$

Where k_0 is the rate constant extrapolated to 0 bar, and $\Delta V^{\neq}$ is the apparent difference between the volume of the reactant state and the transition state and has units of $cm^3\,mol^{-1}$. Only the observed rate constants for R_1, show a significant pressure dependence, with reactive configurations R_2–R_3 giving pressure-independent rate constants within experimental error. Specifically, $\Delta V^{\neq}_{k_1} = -5.7 \pm 1.7$, $\Delta V^{\neq}_{k_2} = 2.4 \pm 3.6$ and $\Delta V^{\neq}_{k_3} = -0.8 \pm 1.3\ cm^3\,mol^{-1}$. The increased conformational freedom in N189A MR that is suggested by our high-pressure MD simulations might explain the smaller pressure dependence of the observed rate of FMN reduction in N189A MR compared to wild-type MR ($\Delta V^{\neq} = 18.3 \pm 0.6\ cm^3\,mol^{-1}$). That is, it seems plausible that increased conformational freedom might "dampen" the effect of high pressure and give smaller values for $\Delta V^{\neq}$. This idea is also supported by the smaller C4–N5 distance decrease that was observed in the molecular dynamics simulations of N189A MR compared to wild-type MR at high pressure.

Pressure dependence of charge-transfer absorption for the N189A MR–$NADH_4$ complex supports a conformationally rich energy landscape

We have monitored the change in charge-transfer (CT) absorption across the pressure range of 1 to 2000 bar for the N189A MR–$NADH_4$ complex by using the method we reported recently for wild-type enzyme.[15] The CT complex that is formed prior to hydride transfer with the natural coenzyme (NADH) has a broad absorbance centred at ~555 nm attributed to the π–π interactions between the nicotinamide and flavin isoalloxazine rings. A similar absorption band is produced with the unreactive $NADH_4$ ligand. We formed the CT absorption by mixing the enzyme with a saturating concentration ($> 10 \times K_d$) of the unreactive NADH analogue, $NADH_4$. With wild-type MR, the CT absorbance (ε_{CT}) increases with increasing hydrostatic pressure [$\Delta\varepsilon_{CT} = 0.09 \pm 0.01\ mM^{-1}\,cm^{-1}\,kbar^{-1}$ at 25 °C (Figure 3, inset)].

Based on Mulliken's[16] and latterly Ewald's[17] work with small-molecule systems, we have suggested that increasing pressure shortens the distance between the ring planes of the nicotinamide and isoalloxazine. This shortening of the CT bond (improved overlap of the π–π orbitals) increases the extinction coefficient, ε_{CT}, for the wild-type MR–$NADH_4$ complex.

The reactive configuration R_1 of N189A MR is structurally similar to the CT complex of wild-type MR.[14] Configuration R_1 contributes to the CT spectrum, whereas configurations R_2 and R_3 are not expected to contribute significantly to the CT absorption spectrum based on geometry considerations.[14] That kinetic decay of the CT complex is monoexponential in N189A, whereas hydride transfer is multiexponential, has been used to argue that configurations R_2 and R_3 do not contribute to the CT absorption spectrum.[14] Given this context, we investigated the effects of pressure on the CT absorption properties of the N189A MR–$NADH_4$ complex (Figure 4). Unlike for wild-type MR,

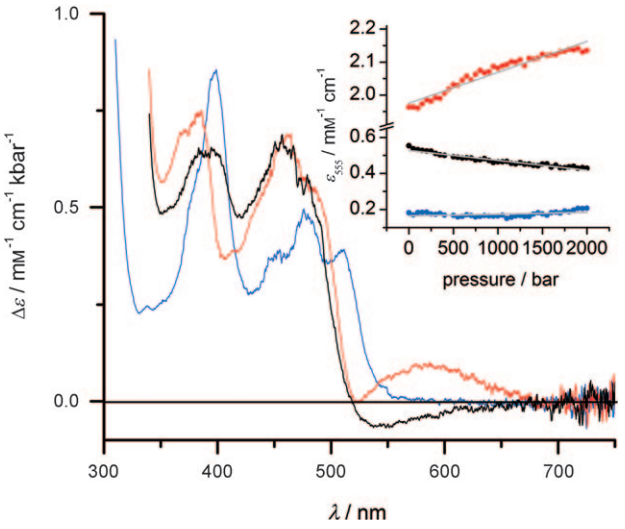

Figure 4. Difference visible absorption spectra (1 kbar minus 1 bar) of $NADH_4$-bound N189A MR (black), $NADH_4$-bound wild-type MR [red, data from Hay et al.,[15] and coenzyme-free N189A MR (blue). The inset shows the pressure dependence of the CT absorbance at 555 nm by using the same colour scheme as the main panel. The solid grey lines show fits to $\varepsilon = \Delta\varepsilon \cdot p + \varepsilon_0$, with $\Delta\varepsilon = -0.09 \pm 0.01$ and $+0.09 \pm 0.01$ $mM^{-1}cm^{-1}kbar^{-1}$ for $NADH_4$-bound N189A MR and wild-type MR, respectively. Conditions: 100 μM N189A MR, 40 mM $NADH_4$ at 4 °C.

where the CT absorption increases with pressure ($\Delta\varepsilon_{CT} = 0.09 \pm 0.01$ $mM^{-1}cm^{-1}kbar^{-1}$), the CT absorption of the N189A MR decreases with pressure ($\Delta\varepsilon_{CT} = -0.09 \pm 0.01$ $mM^{-1}cm^{-1}kbar^{-1}$). A priori, this is inconsistent with our MD simulations, which suggest that the C4–N5 distance decreases at elevated pressure. However, the trend is rationalized by the negative pressure dependence of ΔV_{A1}, which acts to increase the population of configurations R_2 and R_3 (which have no CT absorption) at the expense of configuration R_1, as the pressure is elevated (Figure 3). By using the population decrease for R_1 (44% over the experimental pressure range as assessed from Equation (2); Figure 3) we can estimate the decrease in ε_{CT} attributed to the loss of R_1, being ~0.24 $mM^{-1}cm^{-1}kbar^{-1}$. Consequently, we calculate the approximate pressure dependence of CT absorption intensity for R_1 in the absence of population redistribution (that is, at "fixed" R_1) as $\Delta\varepsilon_{CT} \sim 0.15$ $mM^{-1}cm^{-1}kbar^{-1}$. This value is slightly elevated to that obtained for wild-type MR ($\Delta\varepsilon_{CT} = 0.09 \pm 0.01$ $mM^{-1}cm^{-1}$ $kbar^{-1}$ at 25 °C) and is consistent with closer π–π interaction and the faster hydride transfer kinetics from R_1 (N189A) compared to wild-type enzyme.[14]

Conclusions

Mutation of an enzyme active site can increase the population of conformational states to the extent that they become observable experimentally. We have shown this to be the case in the enzyme–coenzyme complex of MR. We have shown that both kinetic and spectroscopic studies (performed as a function of pressure) point to a multidimensional free-energy landscape in the enzyme–coenzyme complex from which hydride transfer occurs by using parallel chemical pathways. Our work indicates that variable pressure kinetic and spectroscopic studies are useful experimental methods for exploring multidimensional energy landscapes in enzyme catalysis. These approaches might be generally applicable to studies of enzyme mechanism in the analysis of conformational substates that contribute to productive catalysis.

Experimental Section

All materials were obtained from Sigma–Aldrich, except NADH (Melford Laboratories, Chelsworth, UK). Wild-type MR and N189A MR were purified as described previously,[14] and the enzyme concentration was determined by $\varepsilon(462\text{ nm}) = 11.3$ $mM^{-1}cm^{-1}$. As for wild-type MR, the N189A enzyme is stable at room temperature for >12 h as judged by several criteria (retention of full catalytic activity, dynamic light scattering analysis, retention of characteristic FMN absorption spectrum, and the lack of formation of aggregates/precipitation or lack of flavin release from the protein). $NADH_4$ was prepared as described previously.[15] Coenzyme solutions were prepared fresh, and their concentrations were determined by $\varepsilon(340\text{ nm}) = 6.22$ $mM^{-1}cm^{-1}$ (NADH) or $\varepsilon(288\text{ nm}) = 16.8$ $mM^{-1}cm^{-1}$ ($NADH_4$).

Crystals of MR N189A mutant were obtained by using the sitting drop vapour diffusion method at 277K from ~35% PEG 400, 0.1 M Hepes (pH 7.5) and 0.1 M $MgCl_2$, as described previously.[14] Crystals were soaked for approximately 60 s in a 100 mM $NADH_4$ 2.1 M ammonium sulfate solution followed by rapid immersion in oil and flash-cooling in liquid N_2. Diffraction data were collected from a single cryofrozen crystal at Diamond Light Source (Didcot, UK). The data were indexed and integrated by using Mosflm[18] and scaled by using SCALA in CCP4 suite.[19] Refinement and model building were carried out by using Refmac 5[20] and COOT.[21]

Molecular dynamics simulations of wild-type MR and N189A MR were performed under constant-pressure conditions by using AMBER8[22] with the AMBER 03 force field.[23] The structure of wild-type MR was taken from the PDB file 2R14. The structure of N189A MR was built by deleting the carboxamide part of the side chain of Asn189. The initial system setup has been described in detail elsewhere.[14,15] In brief, the final system comprised 31673 atoms for wild-type MR and 31657 atoms for N189A. This includes 357 protein residues, the FMN and NADH cofactors and 18 Na^+ ions to

neutralize the charge, solvated in a truncated octahedral water box by using the TIP3P model with 10 Å between the edge of the box and the protein. This system was first heated to 298K under constant-volume conditions, then equilibrated under constant-pressure conditions (1 bar and 2 kbar) for 2 ns. Production trajectories were collected for 10 ns and these were analysed with PTRAJ, implemented in AMBER8. The NADH-C4–FMN-N5 distance trajectories were also analysed by binning the data at 0.1 Å intervals and fitting these data to a Gaussian.[15]

High-pressure static absorbance measurements and rapid reaction kinetic experiments were both performed with a Hi-Tech Scientific HPSF-56 high-pressure stopped-flow spectrophotometer (TgK Scientific, Bradford on Avon, UK). All reactions at high pressure were performed in 50 mM Tris–HCl, 2 mM 2-mercaptoethanol, pH 8.0 and 5–10 units mL^{-1} glucose oxidase and 50 mM glucose were added for stopped-flow measurements.[13] All stopped-flow experiments were performed with saturating post-mixing concentrations ($>10\times K_d$) of NADH. The conditions that were used confer to pseudo-first-order reaction kinetic behaviour. Spectral changes accompanying FMN reduction were monitored at 466 nm, and rate constants were determined by fitting Equation (1) to stopped-flow transients by using either 1 (wild-type MR) or 4 (N189A MR) exponentials. For N189A MR the fourth exponential was required only for appropriate fitting of the other three.[14] At pressures above 1500 bar, the data were fitted to a double-exponential function as a second slow phase became apparent. This phase had no measurable isotope effect. Rate constants and errors were estimated by taking the standard deviation of 3–6 measurements at each condition.

Acknowledgements

This work was funded by the UK Biotechnology and Biological Sciences Research Council (BBSRC). N.S.S. is a BBSRC Professorial Research Fellow.

Keywords: catalysis · enzymes · flavoproteins · hydride transfer · hydrostatic pressure

[1] A. Ansari, J. Berendzen, S. F. Bowne, H. Frauenfelder, I. E. T. Iben, T. B. Sauke, E. Shyamsunder, R. D. Young, *Proc. Natl. Acad. Sci. USA* **1985**, *82*, 5000–5004.
[2] H. Frauenfelder, *J. Biol. Phys.* **2005**, *31*, 413–416.
[3] P. Senet, G. G. Maisuradze, C. Foulie, P. Delarue, H. A. Scheraga, *Proc. Natl. Acad. Sci. USA* **2008**, *105*, 19708–19713.
[4] J. Shi, B. A. Palfey, J. Dertouzos, K. F. Jensen, A. Gafni, D. Steel, *J. Am. Chem. Soc.* **2004**, *126*, 6914–6922.
[5] N. M. Antikainen, R. D. Smiley, S. J. Benkovic, G. G. Hammes, *Biochemistry* **2005**, *44*, 16835–16843.
[6] W. Min, B. P. English, G. B. Luo, B. J. Cherayil, S. C. Kou, X. S. Xie, *Acc. Chem. Res.* **2005**, *38*, 923–931.
[7] S. Ferrer, I. Tunon, S. Marti, V. Moliner, M. Garcia-Viloca, A. Gonzalez-Lafont, J. M. Lluch, *J. Am. Chem. Soc.* **2006**, *128*, 16851–16863.
[8] I. F. Thorpe, C. L. Brooks, *J. Am. Chem. Soc.* **2005**, *127*, 12997–13006.
[9] S. J. Benkovic, G. G. Hammes, S. Hammes-Schiffer, *Biochemistry* **2008**, *47*, 3317–3321.
[10] Z. X. Liang, T. Lee, K. A. Resing, N. G. Ahn, J. P. Klinman, *Proc. Natl. Acad. Sci. USA* **2004**, *101*, 9556–9561.
[11] J. Basran, R. J. Harris, M. J. Sutcliffe, N. S. Scrutton, *J. Biol. Chem.* **2003**, *278*, 43973–43982.
[12] C. R. Pudney, S. Hay, M. J. Sutcliffe, N. S. Scrutton, *J. Am. Chem. Soc.* **2006**, *128*, 14053–14058.
[13] S. Hay, M. J. Sutcliffe, N. S. Scrutton, *Proc. Natl. Acad. Sci. USA* **2007**, *104*, 507–512.
[14] C. R. Pudney, S. Hay, J. Y. Pang, C. Costello, D. Leys, M. J. Sutcliffe, N. S. Scrutton, *J. Am. Chem. Soc.* **2007**, *129*, 13949–13956.
[15] S. Hay, C. R. Pudney, T. A. McGrory, J. Pang, M. J. Sutcliffe, N. S. Scrutton, *Angew. Chem. Int. Ed.* **2009**, *48*, 1452–1454.
[16] R. S. Mulliken, *J. Am. Chem. Soc.* **1952**, *74*, 811–824.
[17] A. H. Ewald, J. A. Scudder, *J. Phys. Chem.* **1972**, *76*, 249–254.
[18] A. G. W. Leslie, *Joint CCP4 + ESF-EAMCB Newsletter on Protein Crystallography* **1992**, 26.
[19] Z. Otwinowski, W. Minor, *Macromol. Crystallogr. A.* **1997**, *276*, 307–326.
[20] G. N. Murshudov, A. A. Vagin, E. J. Dodson, *Acta Crystallogr. Sect. D Biol. Crystallogr.* **1997**, *53*, 240–255.
[21] P. Emsley, K. Cowtan, *Acta Crystallogr. Sect. D Biol. Crystallogr.* **2004**, *60*, 2126–2132.
[22] D. A. Case, T. E. Cheatham, T. Darden, H. Gohlke, R. Luo, K. M. Merz, A. Onufriev, C. Simmerling, B. Wang, R. J. Woods, *J. Comput. Chem.* **2005**, *26*, 1668–1688.
[23] Y. Duan, C. Wu, S. Chowdhury, M. C. Lee, G. M. Xiong, W. Zhang, R. Yang, P. Cieplak, R. Luo, T. Lee, J. Caldwell, J. M. Wang, P. Kollman, *J. Comput. Chem.* **2003**, *24*, 1999–2012.

Received: February 10, 2009
Published online on April 29, 2009

